C. R. Palevol 16 (2017) 12–26

Contents lists available at ScienceDirect

Comptes Rendus Palevol

www.sciencedirect.com

General Palaeontology, Systematics and Evolution (Vertebrate Palaeontology)

New remains of *Diplocynodon* (Crocodylia: Diplocynodontidae) from the Early Miocene of the Iberian Peninsula

Nouveaux restes de Diplocynodon *(Crocodylia : Diplocynodontidae) du Miocène inférieur de la péninsule Ibérique*

José Luis Díaz Aráez [a], Massimo Delfino [a,b], Àngel H. Luján [a], Josep Fortuny [a,c], Federico Bernardini [c,d], David M. Alba [a,*]

[a] *Institut Català de Paleontologia Miquel Crusafont, Universitat Autònoma de Barcelona, Edifici (ICTA-ICP), Carrer de les Columnes s/n, Campus de la UAB, 08193 Cerdanyola del Vallès, Barcelona, Spain*
[b] *Dipartimento di Scienze della Terra, Università di Torino, Via Valperga Caluso 35, 10125 Torino, Italy*
[c] *Multidisciplinary Laboratory, the 'Abdus Salam' International Centre for Theoretical Physics, Via Beirut 31, 34151 Trieste, Italy*
[d] *Centro Fermi, Museo Storico della Fisica e Centro di Studi e Ricerche "Enrico Fermi", Piazza del Viminale 1, 00184 Roma, Italy*

ARTICLE INFO

Article history:
Received 27 July 2015
Accepted after revision 9 November 2015
Available online 3 June 2016

Handled by Lars van den Hoek Ostende

Keywords:
Fossil crocodiles
Alligatoroidea
Diplocynodon ratelii
Cranial anatomy
Catalonia
Spain

ABSTRACT

We describe crocodylian remains from the Early Miocene (MN4) site of Els Casots (Subirats, Vallès-Penedès Basin, NE of the Iberian Peninsula). Referral to *Diplocynodon* (Alligatoroidea: Diplocynodontidae) is justified by several cranial and postcranial features, including: (1) the subequal and confluent alveoli of the maxilla (fourth and fifth) and dentary (third and fourth); (2) the position of the foramen aëreum on the quadrate; (3) the small and ventrally reflected medial hemicondyle of the quadrate; (4) the distinct dorsoventral step on the frontal; and (5) the bipartite ventral osteoderms. Multiple morphological features are consistent with an attribution to *Diplocynodon ratelii*, previously known from the Early Miocene (MN2) of France, and discount an alternative attribution to other species of the genus, including *Diplocynodon ungeri* from the Middle Miocene (MN5) of Austria. The described material from Els Casots is smaller in size than the French material of *D. ratelii*, possibly reflecting an earlier ontogenetic stage. The described remains constitute the first report of *D. ratelii* and the youngest record of *Diplocynodon* in the Iberian Peninsula, where only *Diplocynodon muelleri* and *Diplocynodon tormis* have been previously reported. The presence of *Diplocynodon* further supports the lacustrine depositional environment previously inferred for Els Casots and also indicates a relatively high temperature.

Mots clés :
Crocodiles fossiles
Alligatoroidea

RÉSUMÉ

Nous décrivons les restes de crocodiliens du site du Miocène inférieur (MN4) d'Els Casots (Subirats, bassin de Vallès-Penedès, Nord-Est de la péninsule Ibérique). Une attribution à *Diplocynodon* (Alligatoroidea : Diplocynodontidae) est justifiée par plusieurs

* Corresponding author.
E-mail address: david.alba@icp.cat (D.M. Alba).

http://dx.doi.org/10.1016/j.crpv.2015.11.003
1631-0683/

Diplocynodon ratelii
Anatomie crânienne
Catalogne
Espagne

caractéristiques crâniennes et postcrâniennes, comprenant : (1) les alvéoles subégales et confluentes du maxillaire (quatrième et cinquième) et dentaires (troisième et quatrième) ; (2) la position du foramen aëreum sur le carré ; (3) l'hémicondyle média du carré, petit et ventralement réfléchi ; (4) l'étape dorsoventrale distincte sur le frontal ; (5) les ostéodermes ventrales bipartites. Plusieurs caractères morphologiques sont compatibles avec une attribution à *Diplocynodon ratelii*, déjà connu au Miocène inférieur (MN2) en France, et permettent de prévoir une attribution alternative à d'autres espèces du genre, y compris *Diplocynodon ungeri* du Miocène moyen (MN5) d'Autriche. Le matériel décrit à Els Casots est de plus petite taille que le matériel français de *D. ratelii*, reflétant probablement un stade ontogénétique antérieur. Les restes décrits constituent le premier rapport sur *D. ratelii* et le plus récent enregistrement de *Diplocynodon* dans la péninsule Ibérique, où seuls *Diplocynodon muelleri* et *Diplocynodon tormis* ont été précédemment signalés. La présence de *Diplocynodon* plaide encore plus en faveur de l'environnement sédimentaire lacustre précédemment inféré pour Els Casots et indique également une température relativement élevée.

1. Introduction

1.1. The site of Els Casots

The paleontological site of Els Casots is located in the municipality of Subirats (Catalonia, Spain), near to the farmhouse of Cal Sutxet (Fig. 1). Although mammalian fossil remains were found in the late 19th century in the nearby lignite mines of Fontsanta (Almera, 1898; Casanovas-Vilar et al., 2011a; Crusafont et al., 1955), it was not until 1989 that new finds led to the discovery of the site of Els Casots (Casanovas-Vilar et al., 2011a; Moyà-Solà and Rius Font, 1993). Excavations carried out there between 1989 and 1994 led to the discovery of abundant small and large vertebrate remains, making Els Casots the most important Early Miocene site from the Vallès-Penedès Basin (Casanovas-Vilar et al., 2011a). The site is also the type locality for two mammal species (Duranthon et al., 1995; Pickford and Moyà-Solà, 1995).

The vertebrate fossil remains from Els Casots include fishes, amphibians, reptiles, birds and micro- and macromammals (Casanovas-Vilar et al., 2011a). Thus far, only a small portion of the recovered material has been prepared and studied in detail, so that despite several previous papers on particular groups, there is no synthetic analysis of the entire fauna. Moyà-Solà and Rius Font (1993) published a preliminary report on the discovery of the site and its fauna, and Agustí and Llenas (1993) provided the first small mammal faunal list from the site. More recently, Casanovas-Vilar et al. (2011a) provided an updated list of mammalian taxa recorded at the site, although detailed studies have focused only on the artiodactyls (Alba et al., 2014; Duranthon et al., 1995; Orliac, 2006; Pickford and Moyà-Solà, 1994, 1995; van der Made, 1997) and certain rodent groups (Aldana Carrasco, 1991, 1992; Ginestí, 2008). Given that almost nothing was known of the non-mammalian vertebrate taxa from Els Casots, a review of the paleoherpetofauna was undertaken by a team from the Institut Català de Paleontologia Miquel Crusafont (ICP). Herein we present the first contribution resulting from this work in progress, a description of the cranial remains of diplocynodontid crocodylians from Els Casots, attributed to *Diplocynodon* Pomel, 1847.

1.2. The fossil record of Diplocynodon

The extinct genus *Diplocynodon*, originally described by Pomel (1847), is considered a European endemic that was distributed widely from the Late Paleocene to the Middle Miocene (Delfino and Smith, 2012; Hua, 2004; Martin, 2010; Martin et al., 2014). Up to nine different species are currently considered taxonomically valid (Delfino and Smith, 2012; Martin, 2010; Martin and Gross, 2011; Martin et al., 2014): *Diplocynodon ratelii* Pomel, 1847 (type species), from the Early Miocene of France (Vaillant, 1872); *Diplocynodon ungeri* (Prangner, 1845), from the Middle Miocene of Austria (Hofmann, 1887a, 1887b) and France (Ginsburg and Bulot, 1997); *Diplocynodon hantoniensis* (Wood, 1846), from the Late Eocene of England and, tentatively (Vignaud et al., 1996), from the Early Oligocene of France; *Diplocynodon darwini* (Ludwig, 1877) and *Diplocynodon deponiae* (Frey et al., 1987), from the Middle Eocene of Germany (Berg, 1966, 1969; Delfino and Smith, 2012); *Diplocynodon muelleri* (Kalin, 1936), from the Middle Oligocene of Spain (Piras and Buscalioni, 2006); *Diplocynodon tormis* Buscalioni et al., 1992, from the Early Eocene to the Early Oligocene of Spain; *Diplocynodon elavericus* Martin, 2010, from the Late Eocene of France (Martin, 2010); and *Diplocynodon remensis* Martin et al., 2014, from the Late Paleocene of France.

According to the results of Delfino and Smith (2012), the basalmost species is *D. darwini*, with the remaining species grouped into two distinct clades: the sister taxa *D. hantoniensis* and *D. ratelii*; and a polytomy between *D. deponiae*, *D. muelleri*, *D. tormis*, and a subclade consisting of *D. elavericus* and *D. ungeri*. Martin et al. (2014) conducted a similar study (based on the same data matrix) that added the oldest species, *D. remensis*. Their analysis also retrieved *D. darwini* as the basalmost species, but followed by a series of nested nodes in the following order (from most basal to most derived): *D. deponiae*, *D. remensis*, *D. hantoniensis*, *D. ratelii*, and the sister taxa *D. muelleri* and *D. tormis*.

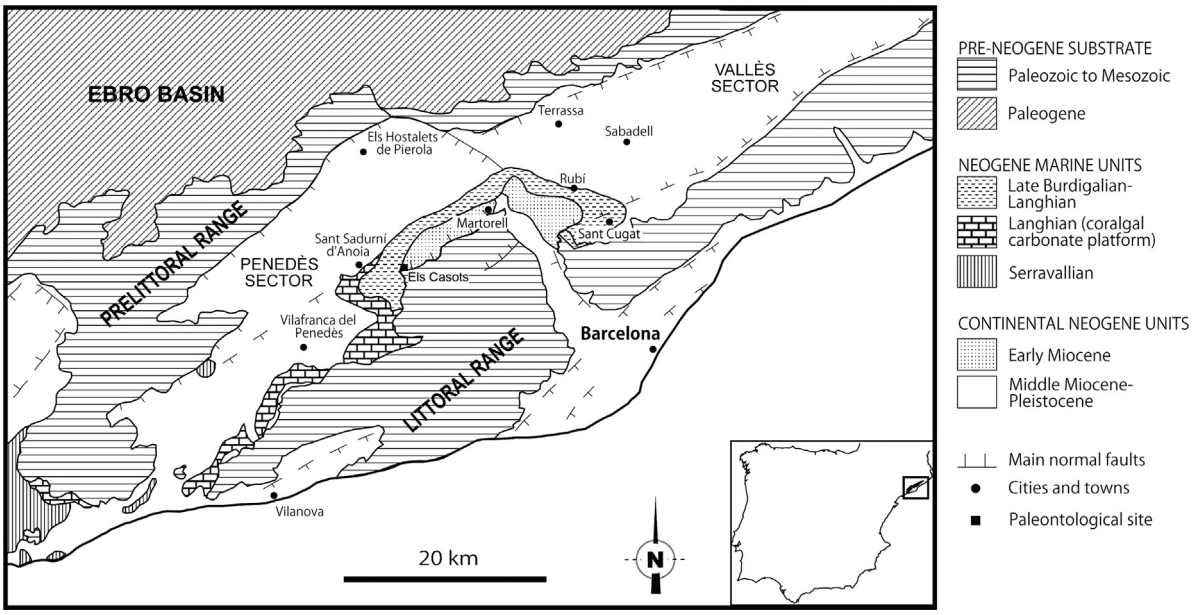

Fig. 1. Schematic geological map of the Vallès-Penedès Basin, showing the location of the site of Els Casots. Modified from Luján et al. (2014).
Fig. 1. Carte géologique schématique du bassin de Vallès-Penedès, montrant l'emplacement du site d'Els Casots. Modifié à partir de Luján et al. (2014).

Diplocynodon is generally considered to have become extinct before the unambiguous dispersal of *Crocodylus* Laurenti, 1768 into Europe toward the Latest Miocene (Delfino et al., 2007). However, the reports (not supported by descriptions) of *Diplonycodon* sp. from several Late Miocene European localities (Böhme and Ilg, 2003), together with the record of cf. *Crocodylus* in the central Mediterranean at 9 Ma (Delfino and Rossi, 2013), might indicate a short coexistence interval between these taxa (Delfino and Rook, 2008; Delfino and Rossi, 2013; Martin and Gross, 2011). As for the two species of *Diplocynodon* previously recorded in the Iberian Peninsula, one of them was originally described by Kalin (1936) as *Hispanochampsa muelleri*, based on Middle Oligocene remains from El Talladell (Tàrrega, Ebro Basin, Catalonia, Spain). Subsequently, this species was reassigned to *Diplocynodon* by Piras and Buscalioni (2006). The other Iberian species is *D. tormis*, which was described by Buscalioni et al. (1992) based on Early Eocene to Early Oligocene remains from various localities of the Salamanca and Zamora provinces (Duero Basin, Spain). The fossils from Els Casots described here, attributed to *D. ratelii*, represent the first remains of *Diplocynodon* from the Vallès-Penedès Basin and the youngest record of the genus in the Iberian Peninsula. Even though *D. ratelii*, the type species of the genus, was established long ago by Pomel (1847), the only thorough description of the material is that provided by Vaillant (1872). Instead, other species of the genus have received much more attention (Delfino and Smith, 2012; Martin, 2010; Martin and Gross, 2011; Martin et al., 2014). Therefore, the descriptions provided here further represent a significant contribution with regard to the morphological diversity of this widespread European genus.

2. Age and geological background

The site of Els Casots is located within the Neogene basin of the Vallès-Penedès (Fig. 1). This basin is an elongated semigraben, oriented parallel to the coastline (E/NE-W/SW) and delimited by the Catalan Coastal Ranges (Littoral and Prelittoral). It originated due to distensive processes associated with the opening of the Valencia Trough during the Late Oligocene-Early Miocene (Agustí et al., 1985; Cabrera et al., 2004; de Gibert and Casanovas-Vilar, 2011; Garcés, 1995). The stratigraphic record of the basin comprises most of the Miocene, beginning at the Ramblian (MN3[1]) and ending in the Late Turolian (MN12; Agustí et al., 1985; Casanovas-Vilar et al., 2011b, 2015). Most of these sediments correspond to continental environments and were deposited in the framework of alluvial fan systems, except by some marine and transitional sediments from the Langhian (roughly equivalent to the Middle Aragonian, MN5; Agustí et al., 1985; Casanovas-Vilar et al., 2011b, 2015).

Els Casots is situated on the southern margin of the basin, being surrounded by small reliefs of Mesozoic carbonates. It is situated within the Lower Continental Complexes of the Vallès-Penedès Basin, which mostly correspond to alluvial deposits (Agustí et al., 1985; de Gibert and Casanovas-Vilar, 2011). However, the locality represents an ancient lacustrine system within the Detritic-Carbonated Unit of Subirats (Cabrera, 1979, 1981; Cabrera et al., 1991; Casanovas-Vilar et al., 2011a), overlying

[1] MN refers to Mammal Neogene units, used in a biostratigraphic sense (see Van Dam, 2003; Hilgen et al., 2012).

Mesozoic deposits (Casanovas-Vilar et al., 2011a; Moyà-Solà and Rius Font, 1993). The stratigraphic succession from Els Casots includes massive limestones corresponding to the center of the lake bottom, a variety of mudstone deposits corresponding to more marginal and shallow areas of the lake, and gravels and conglomerates from the external-most areas.

The age of Els Casots is based on biostratigraphic and lithostratigraphic data, since no magnetostratigraphic data are available (Casanovas-Vilar et al., 2011a). The Detritic-Carbonated Unit of Subirats, to which Els Casots belongs, has been dated to the Early Miocene because it is stratigraphically situated below the marine facies of Middle Miocene age that crop out in the nearby localities of Sant Sadurní d'Anoia and Sant Pau d'Ordal (Cabrera, 1979, 1981; Cabrera et al., 1991; de Gibert and Casanovas-Vilar, 2011). The Detritic-Carbonated Unit of Subirats has been correlated to MN4 based on mammalian biostratigraphy, including the presence of particular cricetodontid and eomyid rodents, deinotheres, the tragulid *Dorcatherium*, the suid *Eurolistriodon* and the bovid *Eotragus* (Agustí et al., 2001; Alba et al., 2014; Casanovas-Vilar et al., 2011a, 2011b). In particular, Els Casots may be correlated to zone C from the Early Aragonian of the Calatayud-Daroca Basin, with an estimated age of 16.5–16.3 Ma, given the presence of *Democricetodon hispanicus* and *Megacricetodon minor primitivus* together with the eomyid *Ligerimys ellipticus* (Casanovas-Vilar et al., 2011a, 2011b).

3. Material and methods

3.1. Studied material

Described specimens. Crocodylian remains at Els Casots are relatively abundant compared to most other Vallès-Penedès localities. However, most of the remains (with the exception of some osteoderms) are not diagnostic even at the family level. These include fragmentary cranial and mandibular bones (IPS9427 to IPS9429, IPS9433, IPS24916, IPS30510a, IPS35078), about 150 teeth (IPS9446a, IPS9447, IPS9450, IPS9451, IPS9554, IPS24148, IPS30510c, IPS35077, and uncatalogued specimens), several vertebral bodies and fragments (IPS9430 to IPS9432, IPS9445, IPS30510b), and 50 osteoderms (IPS9426, IPS9444, IPS30505 to IPS30508, and uncatalogued specimens). Therefore, in this paper we only describe the more diagnostic skull material (IPS951, IPS14721, IPS35073, IPS35074 and IPS30504), as well as the few osteoderms (IPS9426 and IPS9444) that, in a European Miocene context, are diagnostic to the genus rank. All these specimens are housed at the ICP. Comparisons with other species of *Diplocynodon* were based on the literature, with particular emphasis on the data matrix published by Brochu et al. (2012), the most complete matrix available to evaluate the phylogenetic relationships between eusuchians. Character codings based on this data matrix for all species of *Diplocynodon* currently considered valid can be found in Brochu et al. (2012), Delfino and Smith (2012) and Martin et al. (2014). Comparisons of the described material with *D. ratelii* were further complemented by the inspection of specimens from Saint-Gérand-le-Puy (Allier, France) at the MNHN, including two skulls (MNHN SG 539, MNHN SG 13728a), a partial cranium (MNHN SG 541), a partial mandible (MNHN SG 542), and a symphyseal fragment (MNHN SG 543).

3.2. CT scanning

Further preparation of the studied specimens was deemed inappropriate due to their fragility. Therefore, to better ascertain some anatomical details, we decided to undertake a virtual reconstruction of the most informative specimen (IPS951), including an almost complete skull with attached mandible. The fossil was scanned at the Multidisciplinary Laboratory (MLAB) of the Abdus Salam International Centre for Theoretical Physics (ICTP) in Trieste (Italy) using a X-ray microCT system (Tuniz et al., 2013). Due to the size of the specimen and the reduced size of the detector, the skull was scanned in two parts, just changing one of the spatial coordinates: the anterior part of the skull (2047 slices) and the posterior part of the skull (2013 slices). Both parts were scanned under the same parameters (110 kV, 90 μA, an exposure time of 1.2 s and using a 1 mm filter of aluminum), obtaining a pixel resolution of 39.72 μm. The resulting microCT slices were reconstructed using the software DigiXCT in 16-bit format and later digitally segmented (separately for the two parts) using the software Avizo 7.1 (FEI-Visualization Sciences Group Inc.) to remove the matrix. Based on the recorded spatial data, the two 3D models were automatically oriented in their original position by the software, which was then employed to merge them into a single model as well as to digitally separate the cranium from the mandible.

3.3. Measurements

Measurements of the described material, following Martin (2010) and Puértolas-Pascual et al. (2014), were taken with a digital caliper to the nearest 0.1 mm. Most measurements were taken from IPS951, which is the most complete and least deformed specimen, although measurements were also taken from the other specimens when possible.

3.4. Abbreviations

Institutions and fossil collections: ICP: Institut Català de Paleontologia Miquel Crusafont, Universitat Autònoma de Barcelona (Spain); IPS: acronym of the ICP collections (given the former name of the ICP: Institut de Paleontologia de Sabadell); MNHN SG: Muséum national d'Histoire Naturelle, Paris (France), collection from Saint-Gérand-le-Puy.

Anatomical abbreviations: an: angular; art: articular; boc: basioccipital; ch: choanae; d4: fourth dentary alveolus; den: dentary; dss: dorsal splenial suture; dt: dentary tooth; emf: external mandibular fenestra; exo: exoccipital; f: frontal; fa: foramen aëreum; fm: foramen magnum; fs: frontal step; if: incisive foramen; itf: infratemporal fenestra; j: jugal; l: lacrimal; lgsq: longitudinal groove squamosal; lk: longitudinal keel; m: maxillary alveolus; m4: fourth maxillary alveolus; m5: fifth maxillary alveolus;

mg: Meckelian groove; mhq: medial hemicondyle of the quadrate; mx: maxilla; n: nasal; na: naris; oc: occipital condyle; or: orbit; p: parietal; pal: palatine; pf: prefrontal; pm4: fourth premaxillary alveolus; pmx: premaxilla; po: postorbital; pob: postorbital bar; pt: pterygoid; q: quadrate; qj: quadratojugal; soc: supraoccipital; sof: suborbital fenestra; sp: splenial; sq: squamosal; stf: supratemporal fenestra; sur: surangular; vss: ventral splenial suture.

Measurements: ALITF: anteroposterior length of the infratemporal fenestra; ALNA: anteroposterior length of the naris; ALOR: anteroposterior length of the orbit; ALSTF: anteroposterior length of the supratemporal fenestra; AWPOB: anteroposterior width of the postorbital bar; BL: basicranial length between the anterior end of the premaxilla and the posterior end of the occipital condyle; DLPOB: dorsoventral length of the postorbital bar; MCLQ: maximum cranial length between the anterior end of the premaxilla and the posterior end of the quadrate on the sagittal plane; MCWMX: minimum cranial width at the level of the notch between the maxillae and premaxillae; MCWQ: maximum cranial width between the lateral ends of both quadrates; MLCSOC: medial length of the cranium between the anterior end of the premaxilla and the posterior end of the supraoccipital; MLMR: maximum length of the mandibular ramus between the anterior end of the dentary and the posterior end of the retroarticular process; MLS: medial length of the snout between the anterior end of the premaxillae and the level of the anterior end of the orbits; MMW: maximum mandibular width between the posterolateral limits of the angulars; MOW: mediolateral orbital width; MSW: maximum snout width between the anterior ends of both orbits; MPMXW: maximum premaxillary width; MWITF: mediolateral width of the infratemporal fenestra; MWMX: maximum width of the maxilla at the level of the fourth tooth; MWNA: mediolateral width of the naris; MWSTF: mediolateral width of the supratemporal fenestra.

4. Systematic paleontology

Order: Crocodylia Gmelin, 1789
Superfamily: Alligatoroidea Gray, 1844
Family: Diplocynodontidae Hua, 2004
Genus ***Diplocynodon*** Pomel, 1847
Diplocynodon ratelii Pomel, 1847
(Figs. 2–6)

4.1. Preservation of the referred specimens

We provide below an account of the preservation of the specimens described in this paper. Although even the most complete specimens are crushed, distorted and/or still partly covered with matrix, many diagnostic features can be adequately ascertained, as it is clear from the descriptions and figures provided in the following subsection.

IPS951: This specimen is an almost complete skull, with the mandible attached to the cranium in anatomical position (Figs. 2A–D and 3A–D). The skull is dorsoventrally flattened, resulting in some distortion reflected in a dorsal concavity of the snout and dentary (more evident on the right side; Figs. 2C and 3C), as well as a slight displacement of the posterior portion of the mandible towards the right relative to the cranium. The snout is thus depressed due to postdepositional distortion, which is especially apparent in the ventral position of the nasals below the maxillae (Figs. 2C–D and 3C–D). The skull table displays straight margins (Figs. 2A and 3A) and a distinct step on the anterior process of the frontal that is accentuated by dorsoventral compression of the region anterior to the orbits. The cranial cavities of the skull (including the nasal ducts and orbits) as well as some of the mouth cavity are still filled with sediment. However, the virtual 3D models of the cranium and mandible derived from CT scans (Fig. 5A–J, Supplementary Files 1–3) allow us to ascertain additional morphological details. Both premaxillae are complete, including the margins of the foramen incisivum, which display an irregular tear-shaped contour due to compression. The left maxilla is almost complete but very crushed, whereas the right maxilla is more incompletely preserved. The absence of caviconchal recesses on the medial surfaces of the maxillae cannot be ascertained due to dorsoventral compression. The pterygoids, palatines and ectopterygoids are preserved only with very damaged fragments and no hints of sutures or choanae. The lacrimal and prefrontal are visible in dorsal view (Figs. 2A and 3A), but have been crushed and are still covered with sediment. The postorbital bar is broken on the left, and the portion corresponding to the postorbital is hidden by sediment and the depressed postorbital itself (Figs. 2D and 3D). Many teeth are also broken away, damaged or covered by sediment. However, several teeth and tooth fragments remain attached to their respective alveoli, partly due to support by the surrounding matrix still adhered to the skull (Figs. 2B–D and 3B–D). There is a transverse crack through the nasals and maxillae at about mid-length of the snout, where it is more dorsoventrally distorted by compression. This fracture was filled with plaster during preparation, as well as: most of the right maxilla, most of the ventral portions of the maxillae, a small portion of the right premaxilla, a small anterior portion of the right jugal, part of the dentaries, and most of the left angular and surangular (Figs. 2B and 3B).

IPS14721: This specimen is a nearly complete skull with the mandible attached to the ventral portion of the cranium and preserved in a counter-clockwise rotation relative to the correct anatomical position (Figs. 2E–F and 3E–F). The skull is markedly crushed dorsoventrally, and the distal portions of both premaxillae are missing (Figs. 2E and 3E). Both the lacrimal and prefrontal are very deformed, although their sutures can be discerned on the right side. Most of the premaxillary and maxillary alveoli are preserved on the left side, as well as some of the alveoli from the right dentary. The palatine and pterygoid are incompletely preserved and very damaged (Figs. 2F and 3F).

IPS35073: This specimen is represented by a posterior cranial fragment that preserves the skull table, the left orbit, part of the exoccipital and the basioccipital, the left quadrate, left quadratojugal, and portions of the left jugal and right quadrate (Figs. 2G–H and 3G–H). The ornamentation of the cranial bones can be discerned in spite of the presence of some overlying sediment. Most of the preserved bones, except the left quadrate, are quite damaged

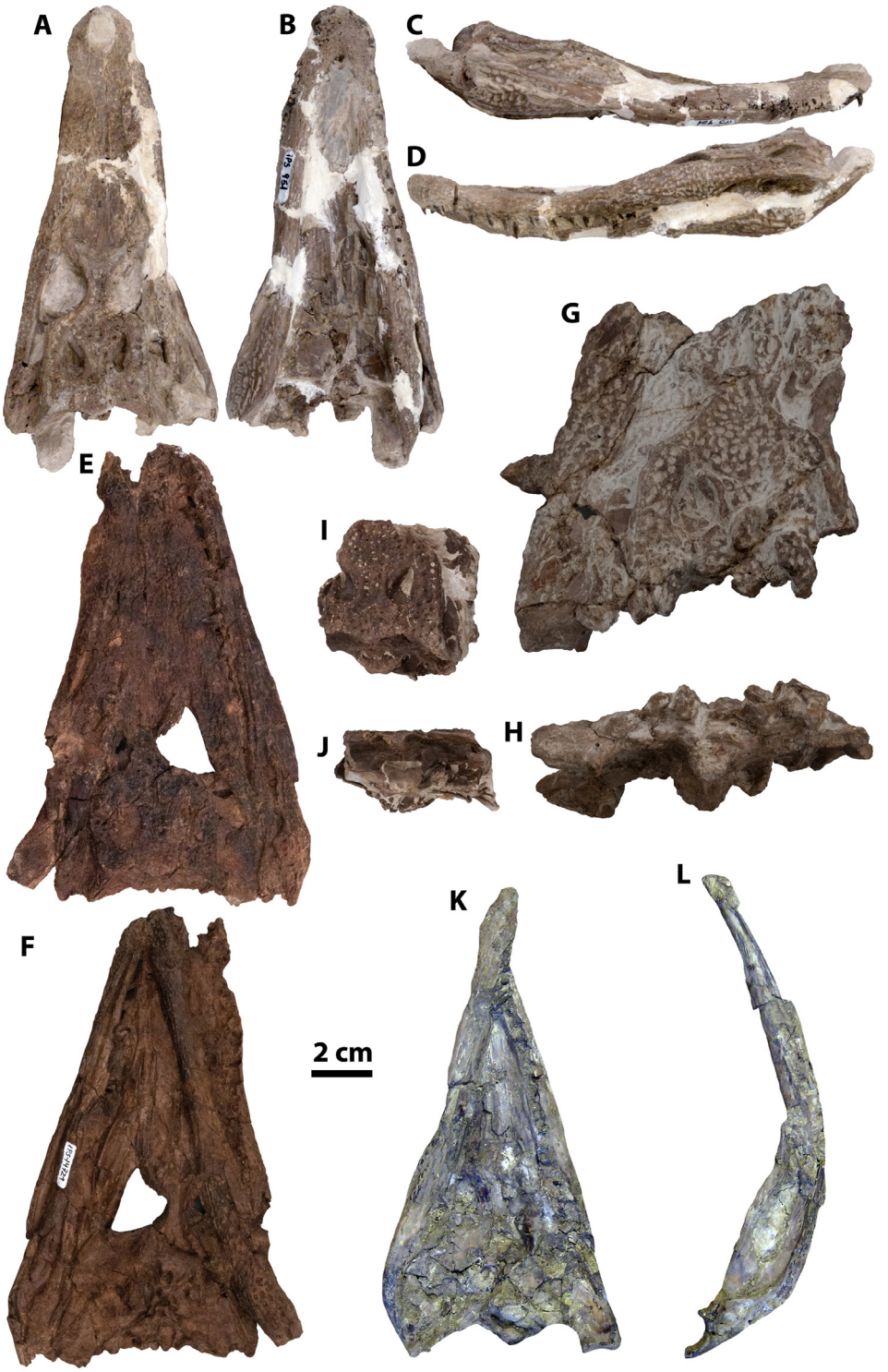

Fig. 2. Fossil remains of *Diplocynodon ratelii* from Els Casots. **A–D**. Skull IPS951, in **A,** dorsal; **B,** ventral; **C,** right lateral; **D,** left lateral views. **E–F**. Skull IPS14721, in **E,** dorsal; **B,** ventral views. **G–H**. Posterior cranial fragment IPS35073, in **A,** dorsal; **B,** posterior views. **I–J**. Posterior cranial fragment IPS35074, in **I,** dorsal; **J,** posterior views. **K–L**. Partial cranium with associated jaws IPS30504, preserved in a rock slab, which was cropped from the photo to ease visualization, in **K,** ventral; **L,** right lateral views.

Fig. 2. Restes fossiles de *Diplocynodon ratelii* d'Els Casots. **A–D**. Crâne IPS951, en vues **A,** dorsale ; **B,** ventrale ; **C,** latérale droite ; **D,** latérale gauche. **E–F**. Crâne IPS14721, en vues **E,** dorsale ; **B,** ventrale. **G–H**. Fragment postérieur du crâne IPS35073, en vues **A,** dorsale ; **B,** postérieure. **I–J**. Fragment postérieur du crâne IPS35074, en vues **I,** dorsale ; **J,** postérieure. **K–L**. Crâne partiel avec hémimandibules associées IPS30504, conservés dans une dalle de roche, qui a été coupée de la photo pour faciliter la visualisation, en vues **K,** ventrale ; **L,** latérale droite.

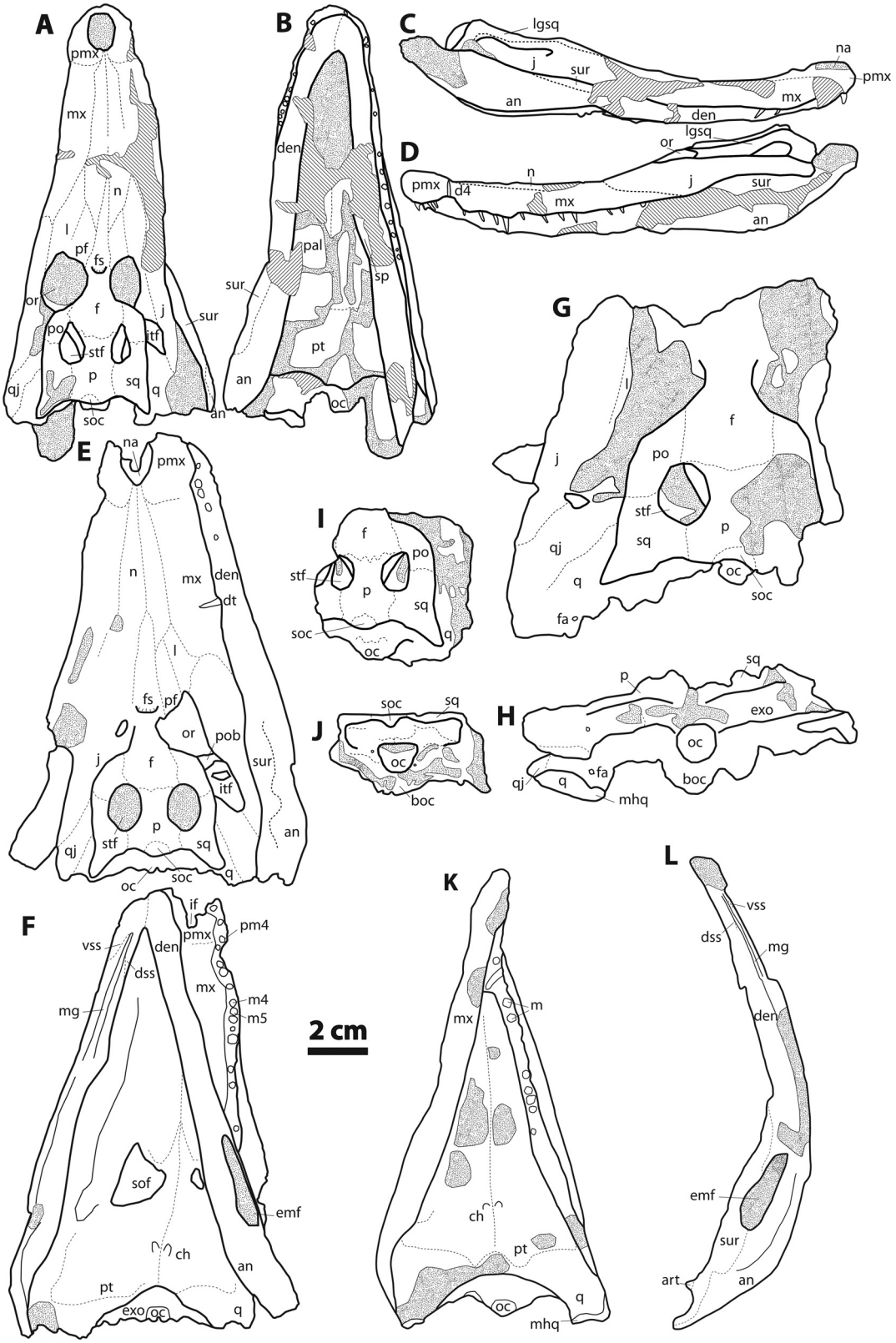

Fig. 3. Schematic drawings of the cranial remains of *Diplocynodon ratelii* from Els Casots reported on Fig. 3. For abbreviations, see § Material and methods.
Fig. 3. Dessins schématiques des restes crâniens de *Diplocynodon ratelii* d'Els Casots rapportés sur la Fig. 3. Pour les abréviations, voir § Matériel et méthodes.

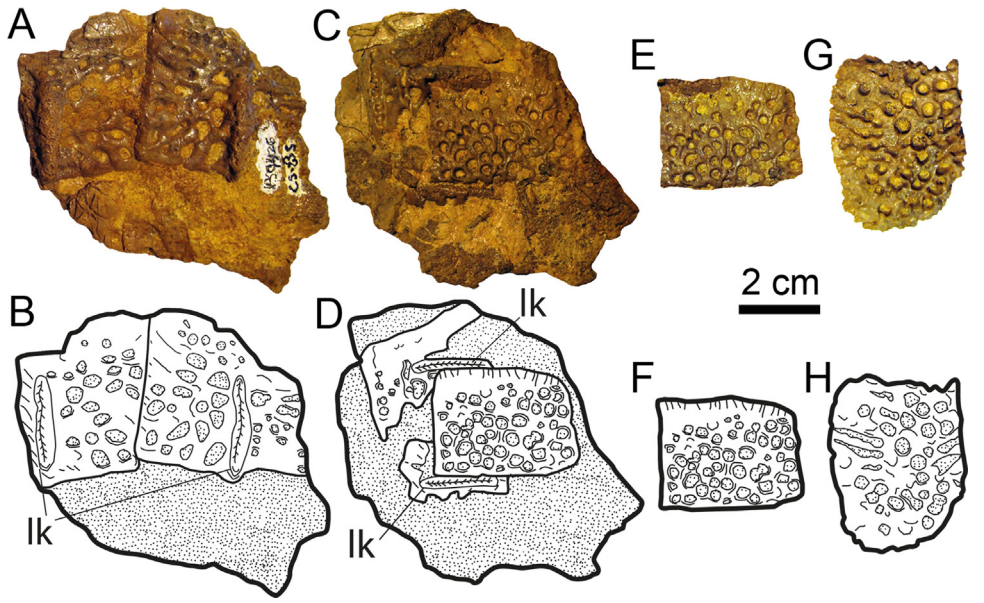

Fig. 4. Photographs (top) and schematic drawings (bottom) of the osteoderms of *Diplocynodon ratelii* from Els Casots. **A–F**. Block with five osteoderms IPS9426: **A–B,** two partial articulated dorsal osteoderms, in external view; **C–D,** two partial dorsal osteoderms and associated ventral bipartite osteoderm, in external view; **E–F,** detailed view of ventral bipartite osteoderm, in external view. **G–H**. Posterior portion of a ventral bipartite osteoderm IPS9444, in external view. For abbreviations, see § Material and methods.

Fig. 4. Photographies (en haut) et dessins schématiques (en bas) des ostéodermes de *Diplocynodon ratelii* d'Els Casots. **A–F**. Bloc avec cinq ostéodermes IPS9426 : **A–B,** deux ostéodermes dorsaux articulés en vue externe ; **C–D,** deux ostéodermes dorsaux partiels et ostéoderme bipartite ventral associé, en vue externe ; **E–F,** vue détaillée d'un ostéoderme bipartite ventral, en vue externe. **G–H**. Partie postérieure d'un ostéoderme bipartite ventral IPS9444, en vue externe. Pour les abréviations, voir § Matériel et méthodes.

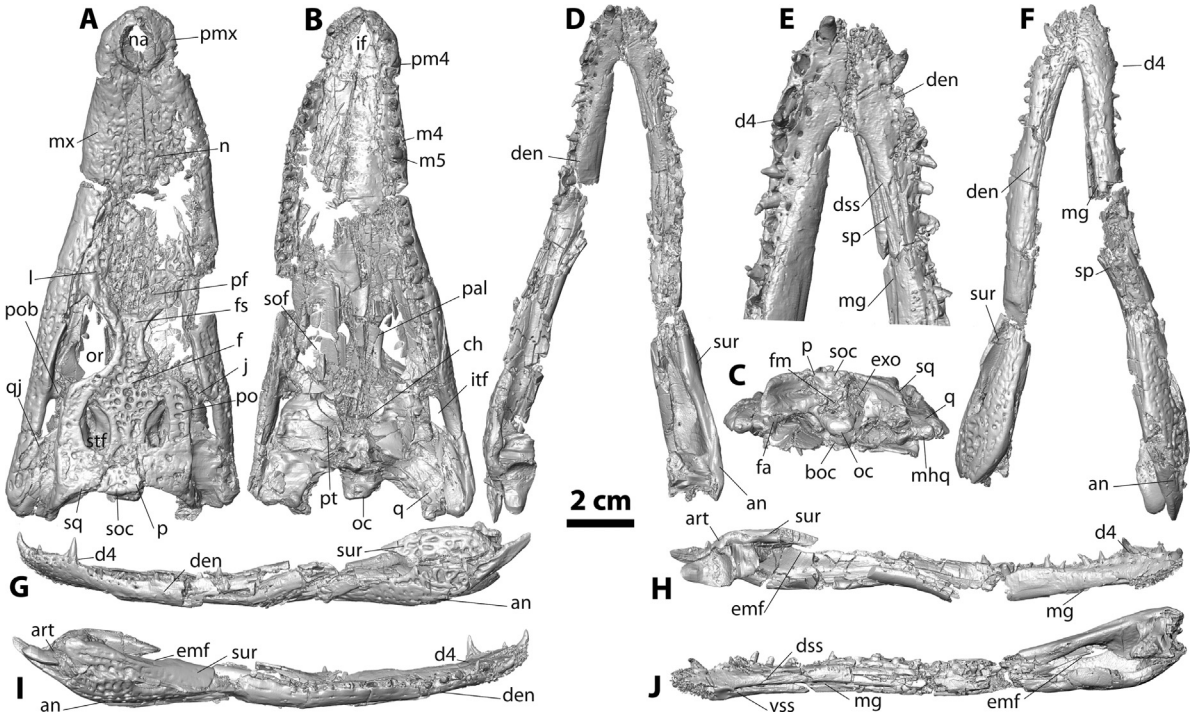

Fig. 5. Digital rendering derived from CT data of the skull IPS951 of *Diplocynodon ratelii* from Els Casots. **A–C**. Cranium in **A,** dorsal; **B,** ventral; **C,** posterior views. **D–J**. Mandible in **D, E,** dorsal (**E** shows a detail of the dentary symphysis); **F,** ventral; **G, I,** labial; **H, J,** lingual views. See Supplementary Files 1–3 for virtual 3D models of the same specimen. For abbreviations, see § Material and methods.

Fig. 5. Rendu numérique dérivé des données CT du crâne IPS951 de *Diplocynodon ratelii* d'Els Casots. **A–C**. Crâne en vues **A,** dorsale ; **B,** ventrale ; **C,** postérieure. **D–J**. Mandibule en vues **D, E,** dorsale (**E** montre un détail de la symphyse dentaire) ; **F,** ventrale ; **G, I,** labiale ; **H, J,** linguale. Voir Fichiers Supplémentaires 1–3 pour des modèles 3D du même spécimen. Pour les abréviations, voir § Matériel et méthodes.

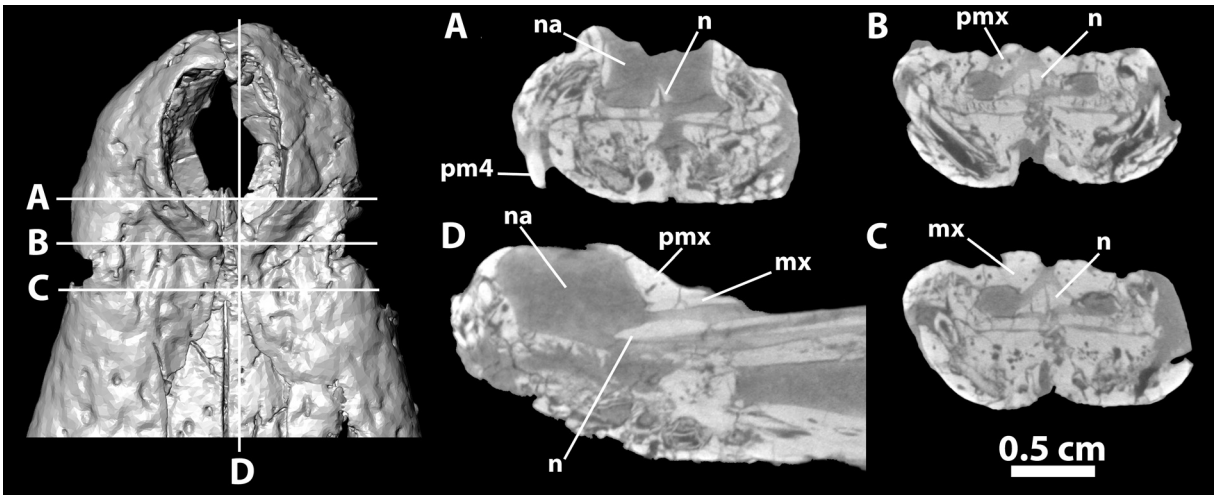

Fig. 6. Digital rendering derived from CT data of the snout of *Diplocynodon ratelii* from Els Casots, showing in detail the contact between the nasals and the premaxillae in IPS951. **A–C**. Coronal sections through the fossa nasalis. **D**. Parasagittal section. See Supplementary Files 1–2 for virtual 3D models of the same specimen. For abbreviations, see § Material and methods.

Fig. 6. Rendu numérique dérivé des données CT du museau de *Diplocynodon ratelii* d'Els Casots, montrant en détail le contact entre les nasaux et les prémaxillaires dans IPS951. **A–C**. Sections coronales à travers la fossa nasalis. **D**. Section parasagittale. Voir Fichiers Supplémentaires 1–2 pour des modèles 3D du même spécimen. Pour les abréviations, voir § Matériel et méthodes.

and fragmentarily preserved due to dorsoventral compression.

IPS35074: This specimen is a posterior cranial fragment that only preserves the skull table, part of the exoccipital and the basioccipital, and other bony fragments that may represent the quadrates and pterygoids (Figs. 2I–J and 3I–J).

IPS30504: This damaged cranial fragment is very crushed, with its dorsal portion still embedded in matrix. It is in direct association with both jaws, which are separated at the symphysis. One of the jaws is close to its original anatomical position, whereas the other is completely disarticulated and preserved away from the rest of the skull (Figs. 2K–L and 3K–L).

IPS9426: This specimen includes four osteoderms preserved within a single block of sediment. On one side, there are two partial dorsal osteoderms, which are almost articulated to one another (Fig. 4A–B). On the other side, there are two partial dorsal osteoderms preserving the longitudinal keel (Fig. 4C–D), and the posterior portion of a ventral bipartite osteoderm (Fig. 4C–F).

IPS9444: This specimen is an isolated posterior half of a ventral osteoderm (Fig. 4G–H).

4.2. Description and measurements

The following description is mostly based on the best-preserved cranium (IPS951; Figs. 2A–D, 3A–D, 6A–D), but further incorporates additional information based on the remaining specimens mentioned above from Els Casots (Figs. 2E–L and 3E–L). Measurements of the described material are reported in Table 1.

Premaxilla: This bone contacts the maxilla posterolaterally and the nasal posteromedially. In IPS951, the premaxilla (which is completely preserved but slightly flattened; Figs. 2A and 3A) displays a round shape anteriorly and is longer than wide (Fig. 6A and D). This bone displays a ridge-like thickening surrounding the naris, which has a slightly oval contour and a shallow concavity on its posterior margin. The premaxillae surround most of the naris, except on its posterior margin, where the nasals reach the naris. The premaxillae thus do not contact each other posteriorly. This can be clearly observed in the 3D model

Table 1
Craniomandibular measurements (in mm) of the specimens of *Diplocynodon ratelii* from Els Casots. Estimated measurements (due to poor preservation) are reported within parentheses, whereas measurements of incompletely preserved specimens are preceded by the symbol '>'. For abbreviations, see Material and methods.

Tableau 1
Mensurations craniomandibulaires (en mm) des spécimens de *Diplocynodon ratelii* d'Els Casots. Mensurations estimées (en raison de la mauvaise conservation) sont signalées entre parenthèses, alors que les mensurations de spécimens conservés incomplètement sont précédées par le symbole « > ». Pour les abréviations, voir Matériels et méthodes.

	IPS951	IPS14721	IPS35073	IPS35074	IPS30504
ALITF	(11.7)	–	(11.2)	–	–
ALNA	13.0	> 12.9	–	–	–
ALOR	(24.7)	(23.5)	(25.9)	–	–
ALSTF	(8.4)	15.1	19.4	14.2	–
AWPOB	3.9	6.9	5.6	–	–
BL	(137.7)	(137.6)	–	–	(147.6)
DLPOB	> 3.8	9.7	12.2	–	–
MCLQ	140.7	(152.3)	–	–	(153.8)
MCWMX	(21.8)	(24.3)	–	–	–
MCWQ	(59.5)	(78.9)	–	–	(71.5)
MLCSOC	133.3	(143.4)	–	–	–
MLMR	147.4	141.5	–	–	(149.9)
MLS	80.1	(81.8)	–	–	–
MMW	(63.0)	–	–	–	–
MWITF	(5.5)	–	(12.1)	–	–
MOW	(14.6)	(15.9)	(19.7)	–	–
MSW	(24.6)	(54.8)	–	–	(51.6)
MPMXW	(22.2)	(29.4)	–	–	–
MWMX	33.0	(43.0)	–	–	–
MWNA	8.7	(6.9)	–	–	–
MWSTF	(14.9)	7.9	16.2	11.2	–

of the skull (Fig. 5A), in which the sediment infill of the naris has been digitally removed (Fig. 6A and D). The posterior margin of the premaxilla is irregular and elongate, progressively narrowing posteriorly and ending with an acute tip between the maxilla and the nasal. In the digital rendering of the CT scans, on the ventral surface of the cranium the premaxilla-maxilla suture is distinctly zigzagging but overall approximately straight and tranverse (Fig. 5B; Supplementary File 2). From the virtual model, it is clear that the posterior dorsal extent of the premaxillae reaches the level of the third maxillary alveoli (Fig. 5B). Also in IPS14721, the posterior end of the premaxilla apparently reaches the third maxillary alveolus (Fig. 3F). In IPS951, the number of premaxillary tooth positions cannot be confidently estimated due to the close proximity of the dentary, although the virtual rendering indicates the presence of five premaxillary tooth positions.

Maxilla: In IPS951, the maxilla is much longer than wide and displays a slight narrowing on its posterior margin (Figs. 2A and 3A). A constriction can be discerned in dorsal view on the left side at the limit between the maxilla and the premaxilla, bisected by the suture between these bones. The course of the premaxillary–maxillary suture can be discerned in IPS14721. This suture divides the above-mentioned notch (Fig. 3E), which would have been occupied by the third and fourth dentary teeth, as it can be observed in the virtual model of IPS951 (Fig. 5B). This constriction appears larger in IPS14721, possibly due to distortion, in which it would have been occupied by the third and fourth dentary teeth. The maxillary teeth in IPS951 are well preserved in their corresponding alveoli on the left side, whereas on the right they are broken away, fragmentary, embedded in matrix or hidden by the displaced dentary, thus preventing a direct count of the total number of maxillary teeth. However, the virtual model shows, on the left side, up to 16 tooth positions (Fig. 5B). The model further shows that the fourth and fifth teeth are very close to one another and that their respective alveoli merge to some extent (the fifth one being slightly larger than the fourth). In IPS14721, these alveoli are similar in size, but due to preservational reasons it is not possible to confirm that they were confluent (Figs. 2F and 3F).

Nasal: This bone contacts the premaxilla anterolaterally, the maxilla laterally, the lacrimal and the prefrontal posterolaterally, and the frontal posteromedially. In IPS951, the nasal is elongate with acute anterior and posterior ends (Figs. 2A and 3A). The anterior ends of both nasals progressively narrow as they pass between the premaxillae (Fig. 6A and D). The posterior end becomes wider laterally all along the contact with the lacrimal and shows a narrow medial extension between the prefrontal and the frontal (Fig. 3A). The virtual model of IPS951 (Fig. 5A and B) clearly shows that the nasals reach the posterior rim of the external naris (Fig. 3A), thus preventing the premaxillae from contacting each other posteriorly. This can also be seen in IPS14721, although less clearly, by close inspection of the preserved sutures (Fig. 3E). In IPS951, the nasal broadens posteriorly up to the point in which the suture between the nasals splits and contacts the anterior process of the frontal. Posteriorly from this point, both nasals separate from each other, surrounding the frontal and becoming progressively narrower until ending on their acute posterior margins at both sides of the anterior process of the frontal. Contact between the nasal and the lacrimal is very broad, as shown by IPS951 and IPS14721 (Fig. 3A and E).

Prefrontal and lacrimal: In IPS14721, the lacrimal and prefrontal display a subtriangular shape, very elongated anteroposteriorly and markedly narrow mediolaterally (Figs. 2A, E and 3A, E). The suture between the lacrimal and prefrontal reaches the anteromedial margin of the orbit. The prefrontal contacts the anterior process of the frontal medially, whereas the lacrimal contacts the nasal anteromedially, the jugal posterolaterally and the maxilla anterolaterally (Fig. 3A and E).

Frontal: The frontal contacts the prefrontal and nasal anterolaterally, the postorbital laterally and the parietal posteriorly. This bone is well preserved in IPS951, although fragmentary near its right margin due to compression that resulted in a slight vertical displacement and clockwise rotation relative to the rest of the bone (Figs. 2A and 3A). The frontal displays a subtriangular morphology that is wide posteriorly and narrows anteriorly, up to the divergence point of the prefrontals. On its posterior portion, the frontal is ornamented with subcircular pits, up to 3 mm in diameter, with some pits still filled with sediment. In IPS951, there is a clear distinction between the main body of the frontal and its anterior process, marked by a notable dorsoventral step (Figs. 3A and 5A). The frontal is markedly concave between the orbits, with elevated orbital margins. The length of the anterior process of the frontal is roughly equivalent to half the total length of the frontal, and its anterior-most extent almost reaches the mid-length of the snout (Fig. 3A and E).

Postorbital: This bone meets the squamosal posteriorly, the frontal anteromedially, and the jugal anterolaterally at the postorbital bar. In IPS951, the postorbital displays an elongate and slightly curved shape (Figs. 2A, 3A, 5A). This bone constitutes the posterior orbital margin, the anterolateral margin of the supratemporal fenestra, and the anterodorsal margin of the infratemporal fenestra. In IPS951, the left postorbital is well preserved, including its sutures with the frontal and squamosal, but the right postorbital is distorted resulting in a slightly elevated position relative to the skull table. Due to distortion, the right supratemporal fenestra is transversely compressed. Ornamentation of subcircular pits on the postorbital is apparent despite being largely filled with sediment. The postorbital can be further observed in other specimens (IPS14721, IPS35073 and IPS35074; Fig. 3E, G, I), which agree in morphology with that displayed by IPS951.

Squamosal: This bone contacts the quadrate ventrolaterally, the postorbital anteriorly, and the parietal medially. In IPS951, the squamosal is longer than wide, becoming narrower anteriorly (Figs. 2A, 3A, 5A). The suture between the squamosal and the postorbital reaches the mid-length of the lateral margin of the supratemporal fenestra. This bone displays a massive posterior prong, which is obliquely oriented relative to the posterodorsal margin of the quadrate. The morphology of the squamosal is similar in the remaining specimens (IPS14721, IPS35073 and IPS35074), although in IPS35073 the posterolateral ramus is poorly preserved (Figs. 2E, G, I and 3E, G, I).

There is a longitudinal groove with parallel sides along the lateral margin of the skull table, from the posterolateral limit of the squamosal up to the posterior orbital margin (Figs. 2C–D and 3C–D). The posterior side of the squamosal has a concave surface. Both squamosals are ventrally compressed above the quadratojugal and the quadrate.

Parietal: The parietal contacts the frontal anteriorly, the squamosal posterolaterally and the supraoccipital posteriorly. In IPS951, the parietal is longer than wide, narrowing anteriorly, and its anterior portion corresponds to the dorsal margin of the supratemporal fenestrae (Figs. 2A, 3A, 5A). There is a step between the posterior margins of both supratemporal fenestrae, due to distortion. The frontoparietal suture is very well defined, with a notable posteriorly-directed curve that extends between the anteriomedial margins of the supratemporal fenestrae. In IPS35074, the frontoparietal suture is similarly well defined but displays less curvature than in IPS951 (Figs. 2I and 3I). Both in IPS951 and IPS35074, the parietal displays a marked ornamentation consisting of the same subcircular depressions present in the frontal and postorbital.

Supraoccipital: This bone is well preserved in several specimens (IPS951, IPS14721 and IPS35074; Figs. 2A, E, I and 3A, E, I). It is exposed on the dorsal surface of the skull table, and does not exclude the parietal from reaching the posterior margin of the skull table in any of the specimens. In all instances, the suture between the supraoccipital and the parietal displays an anteriorly convex shape. In both IPS951 and IPS35074 (Figs. 2A, I–J, 3A, I–J, 5C), the supraoccipital is posteriorly round. In IPS951, the margins of the supraoccipital display a subtriangular shape with very round vertices in posterior view (Figs. 2A, 3A, 5C).

Exoccipital: This bone is only poorly preserved in IPS14721 and IPS35073. It has been dorsoventrally compressed such that no additional descriptive details can be provided (Figs. 2F, H and 3F, H).

Basioccipital: This bone contacts the exoccipitals dorsally. In IPS951, this bone is poorly preserved, except for the condylar area, which is semicircular in posterior view. In IPS35073, the condylar area seems somewhat more posteriorly curved than in IPS951, although this is probably attributable to distortion (Figs. 2G–H and 3G–H).

Jugal: This bone contacts the quadratojugal posteriorly, the maxilla anteriorly, the lacrimal anteromedially, and the postorbital along the postorbital bar. In IPS951, the right jugal is very incompletely preserved, but the left one is quite well preserved, enabling identification of sutures with the maxilla and quadratojugal (Figs. 2A, 3A, 5A). The jugal is anteroposteriorly elongate with its greatest vertical thickness near the orbit. Ornamentation of the jugal consists of very distinct subcircular pits. The medial margin of the jugal is joined to the postorbital bar at the confluence point between the jugal and the posterior end of the orbit, so that the jugal constitutes the whole lateral margin of the orbit, whereas the postorbital bar forms the posterior orbital margin. The anterior end of the jugal narrows dorsally and reaches the level of the ninth or tenth maxillary alveolus. The posterior end of the jugal narrows dorsoventrally before terminating anterior to the craniomandibular joint.

Quadratojugal: This bone contacts the quadrate posteromedialy and the jugal anterolaterally. In IPS941, the left quadratojugal is better preserved than the right one, in spite of being slightly fragmentary and compressed (Figs. 2A and 3A). Sutures between the quadratojugal and its two adjacent bones (jugal and quadrate) can be discerned; they are obliquely oriented relative to the left cranial margin and thus diverge from the lateral margin of the skull table. The quadratojugal is elongate, slightly curved, and ornamented dorsally with relatively large subcircular pits. This bone apparently constitutes the posterior margin of the infratemporal fenestra, although this cannot be conclusively ascertained due to the presence of a fracture.

Quadrate: This bone contacts the squamosal medially, the quadratojugal laterally and the exoccipital dorsolaterally. Both quadrates are relatively well preserved in IPS951 (Figs. 2A, B and 3A, B), although most of the left quadrate is hidden by the squamosal prong dorsally and by the mandible ventrally. The right quadrate can be best ascertained in the virtual rendering derived from the CT scans (Fig. 5A). The foramen aëreum is visible in both quadrates, being substantially far from their medial margin; this can be further ascertained in IPS35073 (Figs. 2G, H and 3G, H). The medial hemicondyle of the right quadrate is relatively small and displays a medioventrally angled orientation in IPS35073 (Figs. 2I, J and 3I, J).

Palatine and pterygoid: These bones are only preserved as small fragments in IPS951, still embedded in sediment such that the choanae cannot be observed (Figs. 2B, 3B, 5B). The palatine and pterygoid are similarly damaged in IPS14721, being crushed and very fragmentary (Figs. 2F and 3F).

Dentary: The dentary constitutes most of the mandible and contacts the surangular posterodorsally, the angular posteroventrally, and the splenial medially (Figs. 2C, D, 3C, D, 5D–J). The dentaries converge anteriorly and are partially fused at the dentary symphysis (as determined from the virtual model of IPS951; Fig. 5D–F). In this specimen, the two dentaries are broken and somewhat distorted, and the teeth are hidden below the premaxilla and maxilla (Figs. 2D and 3D). However, thanks to the CT scans, the presence of 13 alveoli can be ascertained on the left dentary of IPS951 (the right one being too incompletely preserved to count the alveoli). On the left side, it can be further assessed that the third and fourth alveoli are confluent and similar in size, as in the right dentary of IPS14721 (Figs. 2F, 3F, 5D, E). Based on the virtual model of IPS951, the dentary symphysis reaches the posterior margin of the fourth alveolus (Fig. 5D and E). External ornamentation of the dentary is comprised of longitudinal grooves.

Splenial: The lateral edge of this bone contacts the dentary, covering the Meckelian groove. The splenial bifurcates at its anterior end. In IPS951, it can be observed in ventral view that on the left side there is a splenial fragment between the two major cracks displayed by the mandible, close to the limit between the dentary and the angular (Figs. 2B, 3B, 5F). In this specimen, the medial surface of the splenial is visible in the CT scans (Fig. 5H and J), whereas in IPS14721, even though the splenial is lacking, the scar of its

suture with the dentary can be observed (Figs. 2F and 3F). The scars of the dorsal and ventral splenial tips are also preserved on the medial surface of the left dentary of IPS30504 (Figs. 2L and 3L). In IPS951 (Fig. 5D, E, J), the ventral end of the splenial is anteriorly longer than the dorsal end. However, neither tip reaches the dentary symphysis, ending at about the level of the interalveolar space between the fourth and fifth dentary alveoli in IPS951 (Fig. 5D and E) and IPS30504 (Figs. 2L and 3L).

Surangular: The surangular articulates with the dentary anteriorly and constitutes the dorsal margin of the external mandibular fenestra. It contacts the angular ventrally and the articular posteromedially. Both surangulars are incompletely preserved and distorted in IPS951 (Figs. 2A–D, 3A–D, 5A–B, D, F–J), the right one being particularly flattened posteriorly due to dorsoventral compression (Fig. 5H). Ornamentation of the surangular is characterized by anteroposterior grooves on the anterior portion and by irregular large pits on the posterior portion. In this specimen, the dorsal margin of the right surangular is smooth and flat, as in IPS14721, whose surangular is very crushed and distorted both on its right and left margins (Figs. 2E, F and 3E, F).

Angular: This bone constitutes the ventral margin of the external mandibular fenestra and contacts the dentary anteriorly, the surangular posterodorsally and the retroarticular process posteriorly. In IPS951, the angular displays an elongated shape that broadens medially and tapers towards its anterior and posterior ends (Figs. 2A–D, 3A–D, 5A–B, D, F–J). The ornamentation of this bone is constituted by large irregular to subcircular pits. The ventral margin of the angular forms an obtuse angle. In posterior view, both angulars are ventromedially tilted because of distortion. The best angular preservation is on the left side of IPS14721 (Figs. 2E, F and 3E, F), despite distortion separating it from the surangular at their suture. This angular is oriented horizontally in ventral view. Its posterior margin is lacking, but the ventral margin of the external mandibular fenestra can be observed. It further displays a marked ornamentation of subcircular to irregular pits.

Articular: This bone contacts the surangular laterally. In IPS951, the medial extension of the left retroarticular process can be observed in ventral view, being located on the posteromedial margin of the angular (Figs. 2B, 3B, 5D, G–I). Because of the poor preservation of the articular, the foramen aëreum is missing, as well as the suture with the surangular. This precludes determining the position of the lingual foramen relative to the articular–surangular suture.

Dentition and occlusal pattern: The CT scans allow the identification of 5 premaxillary alveoli, 16 maxillary alveoli and at least 13 dentary alveoli in IPS951 (Fig. 5B, D, E). Most likely, the number of dentary alveoli was close to that in the premaxilla and maxilla (i.e., 21), but this cannot be verified due to the poor preservation of the posterior portion of the dentaries. In turn, only 14–15 alveoli can be counted on the maxilla of IPS14721 (Figs. 2F and 3F). The teeth preserved in these specimens display a similar conical morphology, with conspicuous mesiodistal carinae and a labial surface that is more convex than the lingual one. Based on the CT scans of IPS951, occlusal pits can be recognized adjacent to the second through seventh alveoli on the left dentary and at the first through third interalveolar spaces of the maxilla (Fig. 5B, D, E). There is also a broader and deeper depression on the left eighth interalveolar space in the maxilla of IPS951 (Fig. 5B) that might represent an occulsal pit.

Osteoderms: The two dorsal osteoderms (IPS9426) display a subrectangular shape (slightly broader mediolaterally than anteroposteriorly long), an external surface ornamented by large rounded pits except for a smooth anterior articular surface, and a well-developed longitudinal dorsal keel that does not reach the anterior edge (Fig. 4A–B). The posterior portion of bipartite ventral osteoderms (IPS9426 and IPS9444) displays a similar morphology and ornamentation, except that it lacks the longitudinal keel and the smooth anterior articulation surface (Fig. 4C–H).

5. Discussion

5.1. Comparisons and taxonomic attribution

The described specimens clearly belong to a brevirostrine crocodylian characterized by the presence of two subequal and confluent alveoli in both the maxilla (fourth and fifth alveoli) and the dentary (third and fourth alveoli); a foramen aëreum placed far from the medial edge of the quadrate; a small, ventrally reflected medial hemicondyle of the quadrate; a distinct step on the anterior process of the frontal; keeled dorsal osteoderms; and bipartite ventral osteoderms. These characters allow us to refer the material to the alligatoroid *Diplocynodon* (e.g., Brochu, 1999; Martin et al., 2014). The most relevant diagnostic features than can be unambiguously assessed in the specimens from Els Casots for comparison with the nine currently recognized species of *Diplocynodon* are: the shape of the frontoparietal suture (character #149 of Brochu et al., 2012); the contour of the naris (character #85 of Brochu et al., 2012); the extension of the dentary symphysis (character #49 of Brochu et al., 2012); the relative positions of the splenial, Meckelian groove, and dentary symphysis (character #54 of Brochu et al., 2012); and the relationship between the nasals and the external naris (character #82 of Brochu et al., 2012). Codings for these characters are provided for *D. ratelii*, *D. hantoniensis*, *D. muelleri*, *D. tormis* and *D. darwini* by Brochu et al. (2012: supplementary information), for *D. deponiae* by Delfino and Smith (2012), and for *D. elavericus*, *D. ungeri* and *D. remensis* by Martin et al. (2014).

The frontoparietal suture between the supratemporal fenestrae can be clearly observed in both IPS591 and IPS35074 (Figs. 2A, E, G, I, 3A, E, G, I, 5A), in which it is neither extremely concavoconvex nor linear, but moderately curved posteriorly. Among *Diplocynodon* species, the concavoconvex frontoparietal suture displayed by the material from Els Casots only resembles the condition of *D. ratelii* and *D. ungeri* (Brochu et al., 2012; Martin et al., 2014), distinguishing the described material from the remaining species of *Diplocynodon* (except *D. elavericus*, which does not have this feature preserved in any specimen).

Two of the described specimens from Els Casots (IPS951 and IPS14721; Figs. 2A, C–E, 3A, C–E, 5A) further display,

in dorsal view, a crest-like thickening on the margin of the external naris. Among the species of *Diplocynodon*, this feature is only displayed by *D. ratelii* and *D. muelleri*. In the data matrix by Brochu et al. (2012), *D. ratelii* was coded in this regard as displaying a smooth margin of the external naris. However, direct inspection of material of *D. ratelii* from Saint-Gérand-le-Puy (France) revealed a crest delimiting the margin of the external naris (e.g., MNHN SG539, MNHN SG541 and MNHN SG13728a). This feature is also found in *D. muelleri*, but not *D. deponiae*, *D. darwini*, *D. hantoniensis*, or *D. remensis* (Brochu et al., 2012; Delfino and Smith, 2012; Martin et al., 2014). The margin of the external naris cannot be evaluated in *D. elavericus*, *D. tormis*, or *D. ungeri* due to preservation (Brochu et al., 2012; Martin et al., 2014). Therefore, this feature further supports attribution to *D. ratelii*, although it does not discount an alternative attribution to *D. elavericus* or *D. ungeri*. The latter two species can be discounted, however, based on symphyseal extension of the dentary to the fourth alveolus in IPS951. For *D. elavericus* and *D. ungeri* (as well as *D. hantonensis* and *D. darwini*) the dentary symphysis instead extends further, to the sixth to eighth alveoli (Brochu et al., 2012; Martin et al., 2014). A shorter symphysis is found in *D. ratelii*, *D. muelleri* and *D. remensis*, reaching the fourth or fifth dentary alveoli (Brochu et al., 2012; Martin et al., 2014), as with the specimen from Els Casots. This feature is not preserved in *D. tormis* or *D. deponiae* (Brochu et al., 2012; Delfino and Smith, 2012).

The sutural scar left by the missing splenial on the medial surface of the dentary of IPS14721 and IPS30504 (Figs. 2F, L and 3F, L), as well as the virtual model of IPS951 (Fig. 5H and J), indicates that the anterior ventral tip of the splenial is longer than the dorsal one, but does not reach the dentary symphysis. With regard to the latter feature, the material from Els Casots resembles most species of *Diplocynodon* except *D. remensis*, in which the splenial participates in the mandibular symphysis (Martin et al., 2014). The described material further differs from *D. muelleri*, in which the splenial is excluded from the symphysis but in which its dorsal tip is longer than the ventral one (Brochu et al., 2012). The splenial condition displayed by the material from Els Casots is also seen in *D. ratelii* (preserved in MNHN SG542 and SG543), *D. ungeri*, *D. darwini*, *D. hantoniensis*, *D. tormis*, *D. elavericus*, and *D. deponiae* (Brochu et al., 2012; Delfino and Smith, 2012; Martin et al., 2014). Therefore, this feature strengthens an attribution to *D. ratelii* and rules out an alternative referral to *D. muelleri*.

Finally, with regard to the relationship between the nasals and the external naris, both the CT scans of IPS951 and the direct inspection of IPS14721 (Figs. 3A, B, 5A, 6A–D) show that the anterior tip of the nasals reach externally (but do not bisect) the posterior rim of the external naris. According to the published data matrices, all species of *Diplocynodon* in which this feature can be ascertained lack contact between the nasals and the posterior edge of the naris (Brochu et al., 2012; Delfino and Smith, 2012; Martin et al., 2014). This excludes *D. elavericus*, for which this feature cannot be evaluated (Martin et al., 2014). Also, there are some reservations as to the morphology of *D. deponiae* due to poor preservation (Delfino and Smith, 2012). Brochu (1997a, 1997b, 1999) and Brochu et al. (2012) were of the opinion that, in the material of *D. ratelii* from Saint-Gérand-le-Puy, the premaxillae originally met at the midline, but had separated post-mortem, exposing the nasals (C. Brochu, pers. comm. to D.M.A.). However, our inspection of *D. ratelii* from this locality (MNHN SG 13728a) suggests that this taxon uniquely differs from the other species of *Diplocynodon* in having nasals that do reach, even if minimally, the external naris (Fig. 7; see also Vaillant, 1872). The extension of the nasal into the external naris can be more clearly ascertained in the material from Els Casots, thus further supporting its assignment to *D. ratelii* and not to any of the other species of *Diplocynodon*.

Fig. 7. Detail of the snout in MNHN SG 13728a, a cranium of *Diplocynodon ratelii* from Saint-Gérand-le-Puy (France), showing that the anterior tip of the nasals externally reaches the posterior edge of the naris.
Fig. 7. Détail du museau au MNHN SG 13728a, un crâne de *Diplocynodon ratelii* de Saint-Gérand-le-Puy (France), montrant que l'extrémité antérieure des nasaux atteint extérieurement le bord postérieur de la narine.

In summary, the described specimens from Els Casots (MN4) possess the diagnostic features of *D. ratelii*, and display conflicting morphology that allows all other recognized species of *Diplocynodon* to be confidently ruled out. Pomel (1847) originally established *D. ratelii* on the basis of fragmentary material from the Allier department in France, and subsequently Vaillant (1872) described more complete remains from the Allier locality of Saint-Gérand-le-Puy. The latter author assigned part of the material to a second species, *Diplocynodon gracile* Vaillant, 1872, which is considered a junior subjective synonym of *D. ratelii* (e.g., Brochu, 1997a). The described material from Els Casots matches very well with the morphology of specimens of *D. ratelii* from Saint-Gérand-le-Puy (France), including the most complete and best preserved specimen, MNHN SG 539. The only notable difference is the smaller size at Els Casots, which may be due to younger ontogenetic stages. In terms of paleobiogeography, Saint-Gérand-le-Puy is relatively close to Els Casots. The new material reported here from the latter locality therefore extends the stratigraphic range and geographic distribution of *D. ratelii* (previously restricted to the MN2 of France) and represents the first

report of *Diplocynodon* from the Vallès-Penedès Basin, as well as its youngest record in the Iberian Peninsula.

5.2. Paleoenvironmental implications

The site of Els Casots is an ancient lacustrine-palustrine system, as shown by sedimentological evidence and the abundant remains of freshwater fishes, amphibians, and the crocodylian remains described here (Casanovas-Vilar et al., 2011a, 2011b). Most of the mammalian taxa recovered from the site have been associated with forested and humid environments, including the cricetodontids *Democricetodon* and *Megacricetodon*, the glirids *Simplomys* and *Pseudodryomys*, the sciurid *Heteroxerus*, the paleochoerid *Taucanamo*, and the cervids *Lagomeryx* and *Procervulus* (Casanovas-Vilar et al., 2011a, 2011b). This is further reinforced by the tragulid *Dorcatherium*, which is thought to have been tightly linked to water (Alba et al., 2014 and references therein). Els Casots has been interpreted as an ancient lake immediately surrounded by relatively densely forested environments (maybe partially flooded), with more open and drier environments nearby (Casanovas-Vilar et al., 2011a, 2011b). The presence of crocodylians at Els Casots supports the presence of permanent water masses, as well as a relatively high mean temperature (Böhme, 2003; Casanovas-Vilar et al., 2011a, 2011b; Delfino and Rossi, 2013).

6. Summary and conclusions

The crocodylian cranial remains from the Early Miocene (MN4) site of Els Casots (Vallès-Penedès Basin) are described and attributed to *Diplocynodon ratelii*, which was previously known only from the Early Miocene (MN2) of France. The only differences between the French material and the newly described specimens correspond to the smaller size of the latter, which is likely attributable to a younger ontogenetic stage. This material therefore represents the first record of this species in the Iberian Peninsula, where only *D. muelleri* and *D. tormis* had been previously reported. The described remains further represent the youngest record of *Diplocynodon* in the Iberian Peninsula, as well as its first report from the Vallès-Penedès Basin. The presence of this freshwater taxon at Els Casots is entirely consistent with the paleoenvironmental reconstruction of the site as a lacustrine depositional setting, as well as the local climate exhibiting a relatively high temperature.

Acknowledgments

This work was funded by the Spanish Ministerio de Economía y Competitividad (CGL2011-28681, and RYC-2009-04533 to D.M.A) and the Generalitat de Catalunya (2014 SGR 416 GRC). M.D. was supported by Fondi di Ateneo – Università di Torino (2013–2014) and by the Synthesys program (grants FR-TAF 967, BE-TAF 4907, and GB-TAF-3097). We thank Jeremy E. Martin for discussing the morphology of *D. ratelii*, G. Paulet for providing literature, Alejandro Pérez Ramos for assistance with the drawings, and Sergio Llàcer for assistance with the processing of the CT scans. We further acknowledge the Editor (M. Laurin) and the two reviewers (C.A. Brochu and A.K. Hastings) for helpful and constructive comments and suggestions that helped us to improve a previous version of this paper.

Appendix A. Supplementary data

Supplementary data associated with this article can be found, in the online version, at http://dx.doi.org/10.1016/j.crpv.2015.11.003.

References

Agustí, J., Llenas, M., 1993. Los roedores del Mioceno inferior de Els Casots (Vallés-Penedés). Nota preliminar. In: Comunicaciones de las IX Jornadas de Paleontología, Málaga, pp. 70–72.
Agustí, J., Cabrera, L., Moyà-Solà, S., 1985. Sinopsis estratigráfica del Neógeno de la fosa del Vallès-Penedès. Paleontol. Evol. 18, 57–84.
Agustí, J., Cabrera, L., Garcés, M., Krijgsman, W., Oms, O., Parés, J.M., 2001. A calibrated mammal scale for the Neogene of western Europe. State of the art. Earth Sci. Rev. 52, 247–260.
Alba, D.M., DeMiguel, D., Morales, J., Sánchez, I.M., Moyà-Solà, S., 2014. New remains of *Dorcatherium crassum* (Artiodactyla: Tragulidae) from the Early Miocene (MN4) of Els Casots (Subirats, Vallès-Penedès Basin). C. R. Palevol 13, 73–86.
Aldana Carrasco, E.J., (PhD. dissertation) 1991. Roedores esciuromorfos del Neógeno de Cataluña. Universitat Autònoma de Barcelona.
Aldana Carrasco, E.J., 1992. Los Sciurinae (Rodentia, Mammalia) del Mioceno de la cuenca del Vallès-Penedès (Cataluña, España). Treb. Mus. Geol. Barc. 2, 69–97.
Almera, J., 1898. Sobre la serie de mamíferos fósiles descubiertos en Cataluña. Mem. R. Acad. Cienc. Art. Barc. 2, 351–357.
Berg, D.E., 1966. Die Krokodile, insbesondere *Asiatosuchus* und aff. *Sebecus*?, aus dem Eozän von Messel bei Darmstadt/Hessen. Abh. Hessis. Landes. Bodenforsch. 52, 1–105.
Berg, D.E., 1969. Characteristic crocodiles of the Paleogene in Europe. Mem. Bur. Rech. Geol. Min. (BRGM) 69, 73–75.
Böhme, M., 2003. The Miocene climatic optimum: evidence from ectothermic vertebrates of central Europe. Palaeogeogr., Palaeoclimatol., Palaeoecol. 195, 389–401.
Böhme, M., Ilg, A., 2003. fosFARbase (accessed 16.11.2015) http://www.wahre-staerke.com/.
Brochu, C.A., (Ph.D. dissertation) 1997a. Phylogenetic systematics and taxonomy of Crocodylia. The University of Texas at Austin (467 p.).
Brochu, C.A., 1997b. Morphology, fossils, divergence timing, and the phylogenetic relationships of *Gavialis*. Syst. Biol. 46, 479–522.
Brochu, C.A., 1999. Phylogenetics, taxonomy, and historical biogeography of Alligatoroidea. J. Vert. Paleontol. 19 (suppl. 2), 9–100.
Brochu, C.A., Parris, D.C., Grandstaff, B.S., Denton Jr., R.K., Gallagher, W.B., 2012. A new species of *Borealosuchus* (Crocodyliformes, Eusuchia) from the Late Cretaceous–Early Paleogene of New Jersey. J. Vert. Paleontol. 32, 105–116.
Buscalioni, A.D., Sanz, J.L., Casanovas, M.L., 1992. A new species of the eusuchian crocodile *Diplocynodon* from the Eocene of Spain. N. Jahrb. Geol. Paläontol. Abh. 187, 1–29.
Cabrera, L., (PhD. dissertation) 1979. Estudio estratigráfico y sedimentológico de los depósitos basales del Mioceno de la Depresión del Vallès-Penedès. Universitat de Barcelona.
Cabrera, L., 1981. Estratigrafía y características sedimentológicas generales de las formaciones continentales de la cuenca del Vallès-Penedès (Barcelona, España). Estud. Geol. 37, 35–43.
Cabrera, L., Calvet, F., Guimerà, J., Permanyer, A., 1991. El registro sedimentario miocénico en los semigrabens del Vallès-Penedès y de El Camp: organización secuencial y relaciones tectónica sedimentación. In: Colombo, F. (Ed.), Libro-Guía Excursión No. 4. In: I Congreso del Grupo Español del Terciario, pp. 1–132.
Cabrera, L., Roca, E., Garcés, M., de Porta, J., 2004. Estratigrafía y evolución tectonosedimentaria oligocena superior-neógena del sector central del margen catalán (Cadena Costero-Catalana). In: Vera, J.A. (Ed.), Geología de España. Sociedad Geológica de España/Instituto Geológico y Minero de España, Madrid, pp. 569–573.
Casanovas-Vilar, I., Alba, D.M., Moyà-Solà, S., 2011a. Parada 1. Panorámica general de la cuenca y yacimiento de Els Casots (Subirats): una fauna

de vertebrados del Aragoniense inferior. Paleontol. Evol. memòria especial núm. 6, 81–88.
Casanovas-Vilar, I., Alba, D.M., Robles, J.M., Moyà-Solà, S., 2011b. Registro paleontológico continental del Mioceno de la cuenca del Vallès-Penedès. Paleontol. Evol. memòria especial núm. 6, 55–80.
Casanovas-Vilar, I., Madern, A., Alba, D.M., Cabrera, L., García-Paredes, I., van den Hoek Ostende, L., DeMiguel, D., Robles, J.M., Furió, M., van Dam, J., Garcés, M., Angelone, C., Moyà-Solà, S., 2015. The Miocene mammal record of the Vallès-Penedès Basin (Catalonia). C. R. Palevol 15, http://dx.doi.org/10.1016/j.crpv.2015.07.004.
Crusafont, M., Villalta, J.F., Truyols, J., 1955. El Burdigaliense continental de la cuenca del Vallès-Penedès. Mem. Com. Inst. Geol. 12, 1–247.
de Gibert, J.M., Casanovas-Vilar, I., 2011. Contexto geológico del Mioceno de la cuenca del Vallès-Penedès. Paleontol. Evol. memòria especial núm. 6, 39–45.
Delfino, M., Rook, L., 2008. African crocodylians in the Late Neogene of Europe. A revision of *Crocodylus bambolii* Ristori, 1890. J. Paleontol. 82, 336–343.
Delfino, M., Rossi, M.A., 2013. Fossil crocodylid remains from Scontrone (Tortonian, southern Italy) and the Late Neogene Mediterranean biogeography of crocodylians. Geobios 46, 25–31.
Delfino, M., Smith, T., 2012. Reappraisal of the morphology and phylogenetic relationships of the Middle Eocene alligatoroid *Diplocynodon deponiae* (Frey, Laemmert, and Riess, 1987) based on a three-dimensional specimen. J. Vert. Paleontol. 32, 1358–1369.
Delfino, M., Böhme, M., Rook, L., 2007. First European evidence for transcontinental dispersal of *Crocodylus* (Late Neogene of southern Italy). Zool. J. Linn. Soc. 149, 293–307.
Duranthon, F., Moyà-Solà, S., Astibia, H., Köhler, M., 1995. *Ampelomeryx ginsburgi* nov. gen., nov. sp. (Artiodactyla, Cervoidea) et la famille des Palaeomerycidae. C. R. Acad. Sci. Paris, Ser. IIa 321, 339–346.
Frey, E., Laemmert, A., Riess, J., 1987. *Baryphracta deponiae* n.g.n.sp. (Reptilia, Crocodylia), ein neues Krokodil aus der Grube Messel bei Darmstadt (Hessen, Bundesrepublik Deutschland). N. Jahrb. Geol. Paläontol. Monats. 1987, 15–26.
Garcés, M., (PhD. dissertation) 1995. Magnetoestratigrafía de las sucesiones del Mioceno Medio y Superior del Vallès Occidental (Depresión del Vallès-Penedès, N.E. de España): Implicaciones biocronológicas y cronoestratigráficas. Universitat de Barcelona.
Ginestí, M., (Master thesis) 2008. Els cricètids del Miocè inferior dels Casots (Subirats, Barcelona). Universitat Autònoma de Barcelona/Universitat de Barcelona.
Ginsburg, L., Bulot, C., 1997. Les *Diplocynodon* (Reptilia, Crocodylia) de l'Orléanien (Miocène inférieur à moyen) de France. Geodiversitas 19, 107–128.
Gmelin, J.F., 1789. Caroli a Linné. Systema Naturae. Tom I. Pars III. George Emmanuel Beer, Leipzig.
Gray, J.E., 1844. Catalogue of Tortoises, Crocodilians and Amphisbaenians in the Collection of the British Museum. British Museum of Natural History, London.
Hilgen, F.J., Lourens, L.J., Van Dam, J.A., 2012. The Neogene period. In: Gradstein, F.M., Ogg, J.G., Schmitz, M., Ogg, G. (Eds.), The Geologic Time Scale 2012. Elsevier, Amsterdam, pp. 923–978.
Hofmann, A., 1887a. Crocodiliden aus dem Miocaen der Steiermark. Beit. Paläontol- Österr. -Ung. Or. 5, 26–35.
Hofmann, A., 1887b. *Crocodilus steineri* von Schönegg und Brunn bei Wiess, Steiermark. Verhand. Kaiser.-Königlich. Geol. Reich. 10, 219.
Hua, S., 2004. Les crocodiliens du Sparnacien (Eocène inférieur) du Quesnoy (Oise, France). Oryctos 5, 57–62.
Kalin, J.A., 1936. Über Skeletanomalien bei Crocodiliden. Zeitsch. Morphol. ökol. Tier. 32, 327–347.
Laurenti, J.N., 1768. Austriaci viennensis specimen medicum, exhibens synopsin reptilium emendatam cum experimentis circa venena et antidota reptilium austriacorum. J.T. de Trattnern, Vienna.
Ludwig, R., 1877. Fossile Crocodiliden aus der Tertiärformation des Mainzer Beckens. Palaeontogr. Suppl. 3, 1–52.
Luján, A.H., Delfino, M., Casanovas-Vilar, I., Alba, D.M., 2014. Taxonomy of subgenus *Temnoclemmys* Bergounioux, 1958 (Testudines: Geoemydidae: Ptychogasterinae) based on new material from the Vallès-Penedès Basin (NE Iberian Peninsula). C. R. Palevol 13, 277–295.
Martin, J.E., 2010. A new species of *Diplocynodon* (Crocodylia, Alligatoroidea) from the Late Eocene of the Massif Central, France, and the evolution of the genus in the climatic context of the Late Paleogene. Geol. Mag. 147, 596–610.
Martin, J.E., Gross, M., 2011. Taxonomic clarification of *Diplocynodon* Pomel, 1847 (Crocodilia) from the Miocene of Styria, Austria. N. Jahrb. Geol. Paläontol. Abh. 261, 177–193.
Martin, J.E., Smith, T., de Lapparent de Broin, F., Escuillié, F., Delfino, M., 2014. Late Palaeocene eusuchian remains from Mont de Berru, France and the origin of the alligatoroid *Diplocynodon*. Zool. J. Linn. Soc. 172, 867–891.
Moyà-Solà, S., Rius Font, L., 1993. El jaciment paleontològic dels Casots (Subirats, Alt Penedès). Trib. Arqueol. 1991, 7–12.
Orliac, M.J., 2006. *Eurolistriodon tenarezensis*, sp. nov., from Montreal-du-Gers (France): implications for the systematics of the European Listriodontinae (Suidae, Mammalia). J. Vert. Paleontol. 26, 967–980.
Pickford, M., Moyà-Solà, S., 1994. *Taucanamo* (Suoidea, Tayassuidae) from the Middle Miocene (MN04a) of Els Casots, Barcelona, Spain. C. R. Acad. Sci. Paris, Ser. II 319, 1569–1575.
Pickford, M., Moyà-Solà, S., 1995. *Eurolistriodon* gen. nov., (Suoidea, Mammalia) from Els Casots, early Middle Miocene, Spain. Proc. Konink. Neder. Akad. Wetensch. 98, 343–360.
Piras, P., Buscalioni, A.D., 2006. *Diplocynodon muelleri* comb. nov., an Oligocene diplocynodontine alligatoroid from Catalonia (Ebro Basin, Lleida province, Spain). J. Vert. Paleontol. 26, 608–620.
Pomel, A., 1847. Note sur des animaux fossiles découverts dans le département de l'Allier. Bull. Soc. geol. France 4, 378–385.
Prangner, E., 1845. Über *Enneodon Ungeri*, ein neues Genus fossiler Saurier aus den Tertiär-Gebilden zu Wies im Marburger Kreise Steiermark's. Steiermärk. Zeits. 8, 114–139.
Puértolas-Pascual, E., Canudo, J.I., Moreno-Azanza, M., 2014. The eusuchian crocodylomorph *Allodaposuchus subjuniperus* sp. nov., a new species from the Latest Cretaceous (Upper Maastrichtian) of Spain. Hist. Biol. 26, 91–109.
Tuniz, C., Bernardini, F., Cicuttin, A., Crespo, M.L., Dreossi, D., Gianoncelli, A., Mancini, L., Mendoza Cuevas, A., Sodini, N., Tromba, G., Zanini, F., Zanolli, C., 2013. The ICTP Elettra X-ray laboratory for cultural heritage and archaeology. Nucl. Instr. Meth. Phys. Res. A 711, 106–110.
Vaillant, L., 1872. Étude zoologique sur les crocodiliens fossiles tertiaires de Saint-Gérand-le-Puy. Ann. Sci. Geol. 3, 1–57.
Van Dam, J.A., 2003. European Neogene mammal chronology: past, present and future. Deinsea 10, 85–95.
van der Made, J., 1997. Systematics and stratigraphy of the genera *Taucanamo* and *Schizochoerus* and a classification of the Palaeochoeridae (Suoidea, Mammalia). Proc. Konink. Ned. Akad. Wetensch. 100, 127–139.
Vignaud, P., Brunet, M., Guevel, B., Jehenne, Y., 1996. Un crâne de *Diplocynodon* (Crocodylomorpha, Alligatoridae) de l'Oligocène inférieur de Dordogne (France). C. R. Acad. Sci. Paris, Ser. IIa 322, 595–601.
Wood, S., 1846. On the discovery of an alligator and several new Mammalia in the Hordwell Cliff: with observations upon the geological phenomena of that locality. Lond. Geol. J. 1, 117–122.